Astronomy & Astrophysics manuscript no. 16251
January 20, 2011
© ESO 2011

Wavelengths and oscillator strengths of Xe II from the UVES spectra of four HgMn stars

K. Yüce[1,2], F. Castelli[1], and S. Hubrig[3]

[1] Istituto Nazionale di Astrofisica, Osservatorio Astronomico di Trieste, Via Tiepolo 11, I-34143 Trieste, Italy
e-mail: yuce@oats.inaf.it
[2] Ankara University, Faculty of Science, Department of Astronomy and Space Sciences, TR-06100, Tandoğan, Ankara, Turkey
[3] Astrophysical Institute Potsdam, An der Sternwarte 16, D-14482 Potsdam, Germany

arXiv:1101.3725v1 [astro-ph.SR] 19 Jan 2011

ABSTRACT

Aims. In spite of large overabundances of Xe II observed in numerous mercury-manganese (HgMn) stars, Xe II oscillator strengths are only available for a very limited number of transitions. As a consequence, several unidentified lines in the spectra of HgMn stars could be due to Xe II. In addition, some predicted Xe II lines are redshifted by about 0.1 Å from stellar unidentified lines, raising the question about the wavelength accuracy of the Xe II line data available in the literature. For these reasons we investigated the Xe II lines lying in the 3900-4521 Å, 4769-7542 Å, and 7660-8000 Å spectral ranges of four well-studied HgMn stars.
Methods. We compared the Xe II wavelengths listed in the NIST database with the position of the lines observed in the high-resolution UVES spectrum of the xenon-overabundant, slowly rotating HgMn stars HR 6000, and we modified them when needed. We derived astrophysical oscillator strengths for all the Xe II observed lines and compared them with the literature values, when available. We checked the stellar atomic data derived from HR 6000 by using them to compute synthetic spectra for three other xenon-overabundant, slowly rotating HgMn stars, HD 71066, 46 Aql, and HD 175640. In this framework, we performed a complete abundance analysis of HD 71066, while we relied on our previous works for the other stars.
Results. We find that all the lines with wavelengths related to the 6d and 7s energy levels have a corresponding unidentified spectral line, blueshifted by the same quantity of about 0.1 Å in all the four stars, so that we identified these lines as coming from Xe II and modified their NIST wavelength value according to the observed stellar value. We find that the Xe II stellar oscillator strengths may differ from one star to another from 0.0 dex to 0.3 dex. We adopted the average of the oscillator strengths derived from the four stars as final astrophysical oscillator strength.

Key words. line:identification-atomic data-stars:atmospheres-stars:chemically peculiar- stars:individual:HR 6000, HD 71066, 46 Aql, HD 175640

1. Introduction

Several studies of mercury-manganese (HgMn) stars have pointed out the presence of xenon with overabundances up to 5 dex relative to the solar value $\log(N_{Xe}/N_{tot})=-9.87$ (Grevesse & Sauval 1998). This is, for instance, the case of κ Cnc and 33 Gem, for which abundances equal to -4.87 ± 0.13 dex and -4.90 ± 0.07 dex were determined by Dworetsky et al. (2008). The xenon overabundance implies the presence of numerous Xe II lines in the spectra of the HgMn stars, but the Xe II transition probabilities are very incomplete, when we compare the large number of transitions listed in the NIST database and the small number of them with an associated $\log gf$-value. As a consequence, the computed spectra do not include numerous Xe II lines, raising the doubt that some unidentified lines could just be due to Xe II. In addition, we noticed that the wavelengths of several Xe II lines are close, but not coincident with the wavelength of some unidentified stellar lines (Castelli & Hubrig 2007), so that we wondered about the accuracy of the wavelength determination from laboratory spectra.

The most complete work on Xe II is that of Hansen & Persson (1987), who analyzed all the published (Boyce 1936; Humphreys 1939) and unpublished Xe II lines from 392 Å to 10220 Å obtained in laboratory by Humphreys and Boyce. In their discussion on the wavelength accuracy, Hansen & Persson (1987) pointed out that the wavelength accuracy for many lines is too low to be satisfactory, mostly owing to the widely varying quality of the experimental data they used. They announced new experimental work to improve the Xe II atomic data. Unfortunately, this work has never been published up to now, all the more so that some preliminary results had indicated that, for the high 6d and 7s levels, there were shifts of about 0.5 cm^{-1} between the energy levels determined from the Humphrey wavelengths and the energy levels determined from the new data. This energy difference corresponds to a difference of 0.1 Å in wavelengths.

Saloman (2004), who performed a critical compilation of all the work on energy levels and wavelengths of Xe II made up to that time, adopted the data from Hansen & Persson (1987) for almost all the lines of the optical region. The Saloman (2004) critical compilation is the one adopted by the NIST database.

To study wavelengths and $\log gf$-values of the Xe II lines having intensities ≥ 100 in the NIST line list, we used UVES spectra of the four xenon overabundant HgMn stars HR 6000, HD 71066, 46 Aql, and HD 175640. They are slowly rotating stars with $v\sin i$ 1.5 $km\,s^{-1}$, 1.5 $km\,s^{-1}$, 1.0 $km\,s^{-1}$, and 2.5 $km\,s^{-1}$, respectively.

Send offprint requests to: K. Yüce

We already performed a complete abundance analysis for HD 175640 (Castelli & Hubrig 2004a)[1] and for HR 6000 and 46 Aql (Castelli et al. 2009)[2]. To be consistent with the other papers, we present here an abundance analysis of HD 71066, which was studied with the same methods as adopted for the other stars. A previous work on HD 71066, related to vertical abundance stratification in HgMn stars, was performed by Thiam et al. (2010), who adopted the same observations as are used in this paper. We note, however, that no mention about Xe II was made in their study.

2. Observations and data reduction

All the stars were observed at the European Southern Observatory (ESO) using the Very Large Telescope Ultraviolet and Visible Echelle Spectrograph (UVES) with a resolving power ranging from 80000 to 110000.

HD 175640 was observed on June 13, 2001 (Castelli & Hubrig 2004a). HR 6000, 46 Aql, and HD 71066 were part of the same observational run (ESO program 076.D-0169(A)). The spectra of HR 6000 were observed on September 19, 2005, those of 46 Aql on October 18, 2005 (Castelli et al., 2009), while the spectra of HD 71066 were taken on October 27, 2005. Because Nunez et al. (2010) found spectral variations in 19 HgMn stars out of a sample of 28 HgMn stars analyzed, we investigate about a possible variability of HD 71066 by comparing the spectrum observed in 2005 with an UVES spectrum observed in April 2004. We did not find any clear indication of variability.

The spectra of the four stars cover the region 3030 − 10000 Å. For HD 175640 there are two gaps at $\lambda\lambda$ 5759 – 5835 Å and 8519 – 8656 Å. For the other three stars, the gaps occur at 4520 – 4769 Å and 7536 – 7660 Å. All the spectra were reduced by the UVES pipeline Data Reduction Software (Ballester et al. 2000). We analyzed flux-calibrated spectra for the 3050-5750 Å region and RED_SCI_POINT spectra for the 5750-9460 Å interval, in that flux-calibrated reduction for the red spectra was not implemented in the pipeline reduction procedure.

The measurement procedures on the spectra of HD 175640, HR 6000, and 46 Aql were described in Castelli & Hubrig (2004a) and Castelli & Hubrig (2007). The spectra of HD 71066 were normalized to the continuum using the IRAF continuum task. The equivalent widths were measured by a Gaussian fitting using the IRAF splot task.

The S/N ratio is different for the different stars. In the spectra of HD 175640, it ranges from 200 in the near UV to 400 in the visual region. It is higher than the S/N of the spectra of the other three stars, which were observed in a different epoch. Furthermore, for each star, it is different in the different spectral intervals. For instance, for HR 6000, it is about 100 in the 5800−6800 Å interval and lowers to about 25 at 7400 Å (REDL spectrum). It is about 50 at 7800 Å and decreases to about 25 at 9400 Å (REDU spectrum). This behavior is similar for 46 Aql and HD 71066. At 6800 Å the S/N is about 100 for HR 6000, 70 for 46 Aql, 100 for HD 71066, and 125 for HD 175640.

3. The HgMn star HD 71066

Previous studies of HD 71066 (κ^2 Vol, HR 3302) have pointed out the isotopic anomaly of Hg (Dolk et al. 2003; Thiam et al. 2010). No vertical abundance stratification for Ti, Cr, and Fe is found by Thiam et al. (2010). No presence of magnetic field is found both from the inspection of the equivalent widths of the Fe II lines at 6147.7 Å and 6149.2 Å (Hubrig et al. 1999) and after using the FORS 1 spectropolarimeter at the VLT (Hubrig et al. 2006).

Table 1. Abundances $\log(N_{elem}/N_{tot})$ for HD 71066.

elem	HD 71066 [12000K,4.1]	Star-Sun	Sun[a]	Thiam et al.(2010) [12010,3.95]
He I	≤ −2.28	≤ [−1.23]	−1.05	−2.30±0.40
Be II	−10.79	[−0.15]	−10.64	
C II	−3.90	[−0.38]	−3.52	−3.89±0.10
N I	≤ −5.50	≤−1.38	−4.12	
O I	−3.61±0.05	[−0.40]	−3.21	−3.61±0.14
Ne I	≤ −4.70	≤[−0.74]	−3.96	
Na I	−5.51 ±0.08	[+0.20]	−5.71	
Mg I	−5.32 ±0.05	[−0.86]	−4.46	
Mg II	−5.40	[−0.94]	−4.46	−5.46±0.01
Al I	≤−7.30	≤[−1.73]	−5.57	
Al II	≤−7.30	≤[−1.73]	−5.57	
Si II	−4.61±0.19	[−0.12]	−4.49	−4.58±0.07
P II	−5.06±0.13	[+1.53]	−6.59	−4.87±0.22
P III	−5.13	[+1.46]	−6.59	
S II	−5.77±0.11	[−1.06]	−4.71	−5.66±0.20
Ca II	−6.50±0.21:	[−0.82]	−5.68	−6.02
Sc II	≤−10.50	≤[−1.63]	−8.87	
Ti II	−6.45±0.06	[+0.57]	−7.02	−6.52±0.05
V II	≤−10.0	≤[−1.96]	−8.04	
Cr II	−6.17±0.06	[+0.20]	−6.37	−6.28±0.09
Mn II	−5.95±0.04	[+0.70]	−6.65	−5.81±0.20
Fe I	−3.85±0.06	[+0.69]	−4.54	−3.98±0.06
Fe II	−3.85±0.13	[+0.69]	−4.54	−3.87±0.14
Co II	≤−7.88	≤[−0.76]	−7.12	
Ni II	≤−7.90	≤[−2.11]	−5.79	
Cu II	≤−7.83	≤[0.00]	−7.83	
Zn II	≤−7.94	≤[−0.5]	−7.44	
As II	−6.3:	+3.37:	−9.67	
Sr II	−8.27	[+0.8]	−9.07	−8.35
Y II	−7.57±0.08	[+2.23]	−9.80	
Xe II	−5.43±0.16	[+4.44]	−9.87	
Nd III	−9.63±0.01	[+0.91]	−10.54	
Dy III	−9.90	[+1.00]	−10.90	
Au II	−7.12±0.03	[+3.91]	−11.03	
Hg I	−6.40	[+4.51]	−10.91	−6.38±0.28
Hg II	−6.40	[+4.51]	−10.91	−6.53±0.33

[a] Solar abundances are from Grevesse & Sauval (1998).

3.1. Model parameters and abundances of HD 71066

The starting model parameters of HD 71066, $T_{\rm eff}$=12045 K, and log g=3.9 were derived both from the Strömgren photometry and the Fe I – Fe II ionization equilibrium constraint.

The observed colors (b−y)=−0.053, m=0.122, c=0.731 β=2.769 were taken from the Hauck & Mermilliod (1998) Catalogue[3]. The synthetic colors were taken from the grid computed by Castelli for [M/H]=0 and microturbulent velocity ξ=0 km sec^{-1} [4]. Zero reddening was adopted for this star, in agreement with the results from the UVBYLIST code of Moon

[1] http://wwwuser.oat.ts.astro.it/castelli/hd175640/hd175640.html
[2] http://wwwuser.oat.ts.astro.it/castelli/hr6000new/hr6000.html
[3] http://obswww.unige.ch/ gcpd/gcpd.html
[4] http://wwwuser.oat.ts.astro.it/castelli/colors/uvbybeta.html

Table 2. The strongest emission lines in HD 71066, with the atomic data and configurations from the Kurucz website (see footnote 5)

λ(Å)	elem	log gf	χ_{low}	J_{low}	lower config.	χ_{up}	J_{up}	upper config.	Rc obs.	Rc comp.
5987.384	Ti II	+0.649	64979.278	3.5	(^{3}F)4d e4G	81676.439	4.5	(^{3}F)4f 2[4]	1.012	0.983
6001.400	Ti II	+0.724	65095.972	4.5	(^{3}F)4d e4G	81754.137	5.5	(^{3}F)4f 2[5]	1.012	0.981
6029.278	Ti II	+0.653	65308.434	4.5	(^{3}F)4d e4H	81889.576	5.5	(^{3}F)4f 3[6]	1.025	0.984
6125.861	Mn II	+0.788	82144.480	3.0	(^{6}S)4d e5D	98464.200	4.0	(^{6}S)4f ^{5}F	1.023	0.896
6181.354	Cr II	+0.184	89812.420	2.5	(^{5}D)4d f4D	105985.630	3.5	(^{5}D)4f 4[4]	1.010	0.996
6182.340	Cr II	+0.402	89336.890	2.5	(^{5}D)4d e4P	105507.520	3.5	(^{5}D)4f 2[3]	1.015	0.992
6285.601	Cr II	−0.229	89885.080	3.5	(^{5}D)4d f4D	105790.060	4.5	(^{5}D)4f ^{4}F	1.011	0.998
6526.302	Cr II	+0.253	89885.080	3.5	(^{5}D)4d f4D	105203.460	4.5	(^{3}F)sp r^{4}F	1.010	0.996
6551.373	Cr II	+0.201	90725.870	3.5	(^{5}D)4d e4F	105985.630	3.5	(^{5}D)4f 4[4]	1.018	0.997
6585.241	Cr II	+0.815	90850.960	4.5	(^{5}D)4d e4F	106032.240	5.5	(^{5}D)4f 4[6]	1.028	0.987
6592.341	Cr II	+0.287	90512.560	1.5	(^{5}D)4d e4F	105677.490	2.5	(^{5}D)4f 3[3]	1.014	0.996
6636.427	Cr II	+0.573	90725.870	3.5	(^{5}D)4d e4F	105790.060	4.5	(^{5}D)4f ^{4}F	1.020	0.992
6961.439	Ti II	+0.663	67822.582	4.5	(^{3}F)4d e2G	82183.467	5.5	(^{3}F)4f 4[6]	1.025	0.991
6982.307	Ti II	+0.401	67606.162	3.5	(^{3}F)4d e2G	81924.126	4.5	(^{3}F)4f 3[4]	1.015	0.995
8335.148	C I	−0.437	61981.820	1.0	p3s ^{1}P	73975.910	0.0	p3p ^{1}S	1.023	0.889
9405.730	C I	+0.285	61981.820	1.0	r3s ^{1}P	72610.720	2.0	p3p ^{1}D	1.088	0.730

Table 3. The isotopic mixture (IM) (in %) of Hg in HD 71066 from the Hg II line at 3984 Å as derived by us , Dolk et al. (2003) (DWH), and Thiam et al.(2010) (TLKW)

isotope	λ(Å)	IM	log(IM)	IM	IM
		this work		DWH	TLK
196	3983.771	0.5	−2.30	0.1±0.1	1.1
198	3983.839	0.5	−2.30	0.1±0.2	4.0
199a	3983.844	0.5	−2.30	0.1±0.2	3.4
199b	3983.853	0.5	−2.30	0.1±0.2	3.4
200	3983.912	0.5	−2.30	0.1±0.1	15.2
201a	3983.932	0.5	−2.30	0.1±0.3	66.9
201b	3983.941	0.5	−2.30	0.1±0.3	66.9
202	3983.993	2.5	−1.60	1.5±0.3	8.1
204	3984.072	95.0	−0.022	98.0±1.5	1.3

(1985). Observed c and β indices are reproduced by synthetic indices for model parameters $T_{\rm eff}$=12045 K and log g=3.9

The parameters from the photometry were used for computing an ATLAS9 model with solar abundances for all the elements and zero microturbulent velocity. Using the WIDTH code (Kurucz 2005), we derived the Fe I and Fe II abundance from the equivalent widths of 12 Fe I lines and 26 Fe II lines. Seven of the Fe II lines are transitions between high-excitation energy levels, and they have experimental log gf-values. They were used to determine the iron abundance, in that they are rather independent of $T_{\rm eff}$ and log g (Castelli et al., 2009). Then, we searched for the model atmosphere giving this same abundance from both Fe I lines and low-excitation Fe II lines. All the adopted lines are listed in Table A.1 of Appendix A (online material). We find that the ATLAS9 model with the parameters $T_{\rm eff}$=12045 K, log g=3.9 derived from the Strömgren photometry meets the requirement of same iron abundance from all the different kinds of iron lines. In fact, it gives an average abundance log(N(Fe)/N$_{tot}$) equal to −3.88±0.08 from the Fe I lines, −3.92±0.12 from the low-excitation Fe II lines, and −3.84±0.05 from the Fe II high-excitation lines.

The ATLAS9 model was used to derive the abundance for all those elements that show lines in the synthetic spectrum when solar abundance is adopted for them. Whenever possible, equivalent widths were measured to derive the abundances. For weak and blended lines and for lines that are blends of transitions belonging to the same multiplet, such as Mg II 4481 Å, He I lines, and most O I profiles, we derived the abundance from the line profiles. The synthetic spectrum was also used to determine upper abundance limits from those lines predicted for solar abundances, but not observed.

The SYNTHE code, together with updated Kurucz line lists (Castelli & Hubrig 2004a; Castelli & Kurucz 2010), were used to compute the synthetic spectrum. The synthetic spectrum was broadened for the instrumental profile and for a rotational velocity $vsini$=1.5 km s^{-1}, which was derived from the comparison of the observed and computed profile of Mg II at 4481 Å.

Once all the abundances had been determined in this way, we computed an ATLAS12 model for the individual abundances having the same parameters as the ATLAS9 model. We used the seven Fe II high-excitation lines to determine the new iron abundance. The ATLAS12 parameters were then modified until obtaining the same iron abundance, within the error limits, from both the Fe I lines and the low-excitation Fe II lines. The average iron abundances from Fe I, Fe II low-excitation, and Fe II high-excitation lines are −3.85±0.07, −3.87±0.12, and −3.81±0.05, respectively, for an ATLAS12 model with parameters $T_{\rm eff}$=12000 K and log g=4.1. This model also leads to good agreement between the observed and computed H$_\alpha$ profiles. The abundances of HD 71066 derived from the ATLAS12 model either from equivalent widths or line profiles are listed in Table 1.

We also see As II lines at 4466.348 (weak), 4494.23 (weak), 5105.58, 5231.38, 5331.23, 5497.727, 5558.09, 5651.32, 6110.07, and 6170.27 Å were observed in the spectrum. Owing to the lack of log gf-values for all the optical As II transitions, we can only infer overabundance of this element in HD 71066. A guessed abundance of −6.3 dex for arsenic was derived from measured equivalent widths and from guessed log gf-values (Table A.1 and Table 1).

In addition to the overabundance of arsenic and to the large overabundance of iron ([+0.69]), overabundances of P ([+1.5]), Na ([+0.2]), Ti ([+0.6]), Cr ([+0.2]), Mn ([+0.7]), Sr ([+0.8]), Y([+2.2]), Xe ([+4.4]), Nd([+0.9]), Dy ([+1.0], Au ([+3.9]), and Hg ([+4.5]) were observed. The other elements - He, Be, C ,N, O, Ne, Mg, Al, Si, S, Ca, S, V, Co, Ni, Cu, and Zn - are underabundant.

Table 4. Atomic data for selected Xe II lines

λ(Ritz)	Int.	χ_{low}	Term		χ_{up}	Term		log gf	$log(\gamma_S/\mathrm{Ne})(\mathrm{cm^3\,s^{-1}})$	
(Å)		(cm^{-1})			(cm^{-1})			NIST	Dj	PD
4844.32	2000	93068.44	$(^3P_2)6s$	$[2]_{5/2}$	113705.40	$(^3P_2)6p$	$[3]_{7/2}$	+0.491	−5.347	−5.420
5292.21	1000	93068.44	$(^3P_2)6s$	$[2]_{5/2}$	111958.89	$(^3P_2)6p$	$[2]_{5/2}$	+0.351	−5.482	−5.450
5419.14	2000	95064.38	$(^3P_2)6s$	$[2]_{3/2}$	113512.36	$(^3P_2)6p$	$[3]_{5/2}$	+0.215	−5.481	−5.518
5438.97	400	102799.07	$(^3P_1)6s$	$[1]_{3/2}$	121179.80	$(^3P_1)6p$	$[0]_{1/2}$	−0.183	−5.544	−5.369
5472.61	500	95437.67	$(^3P_2)5d$	$[3]_{7/2}$	113705.40	$(^3P_2)6p$	$[3]_{7/2}$	−0.449	−5.482	
5531.06	400	95437.67	$(^3P_2)5d$	$[3]_{7/2}$	113512.36	$(^3P_2)6p$	$[3]_{5/2}$	−0.616	−5.504	
5719.61	200	96033.48	$(^3P_2)5d$	$[2]_{3/2}$	113512.36	$(^3P_2)6p$	$[3]_{5/2}$	−0.746		
5976.46	1000	95064.38	$(^3P_2)6s$	$[2]_{3/2}$	111792.17	$(^3P_2)6p$	$[2]_{3/2}$	−0.222	−5.545	−5.556
6036.20	500	95396.74	$(^3P_2)5d$	$[2]_{5/2}$	111958.89	$(^3P_2)6p$	$[2]_{5/2}$	−0.609	−5.535	
6051.15	1000	95437.67	$(^3P_2)5d$	$[3]_{7/2}$	111958.89	$(^3P_2)6p$	$[2]_{5/2}$	−0.252	−5.515	
6097.59	1000	95396.74	$(^3P_2)5d$	$[2]_{5/2}$	111792.17	$(^3P_2)6p$	$[2]_{3/2}$	−0.237		
6990.88	2000	99404.99	$(^3P_2)5d$	$[4]_{9/2}$	113705.40	$(^3P_2)6p$	$[3]_{7/2}$	+0.200		−5.476

Table 5. Xenon abundance from the measured equivalent widths of HR 6000, 46 Aql, HD 71066, and HD 175640, for each star, using ATLAS12 models with parameters $T_{\rm eff}$ and log g given in the table.

[$T_{\rm eff}$,log g]	HR 6000 [13450,4.40]		HD 71066 [12000,4.10]		46 Aql [12560,3.80]		HD 175640 [12000,3.95]	
λ(Å)	W(mÅ)	abund	W(mÅ)	abund	W(mÅ)	abund	W(mÅ)	abund
4844.33	28.80	−5.10	20.72	−5.21	17.94	−5.67	11.33	−5.86
5292.21	30.19	−4.98	19.72	−5.20	16.52	−5.63	10.80	−5.81
5419.14	23.63	−5.02	14.27	−5.24	13.34	−5.56	7.75	−5.80
5438.97	5.71	−5.42	2.93	−5.55	2.59	−5.85	−−	−−
5472.61	7.56	−5.34	5.03	−5.34	2.85	−5.90	−−	−−
5531.06	4.13	−5.52	1.87	−5.71	2.05	−5.89	−−	−−
5719.61	4.29	−5.30	1.40	−5.64	−−	−−	1.79	−5.58
5976.46	11.34	−5.18	4.74	−5.49	3.43	−5.93	1.60	−6.15
6036.20	6.74	−5.14	2.44	−5.45	2.31	−5.73	−−	−−
6051.15	9.56	−5.25	4.59	−5.44	3.65	−5.84	1.46	−6.13
6097.59	6.79	−5.49	3.93	−5.53	2.57	−6.03	1.94	−5.99
6990.88	11.20	−5.18	5.18	−5.36	5.59	−5.61	2.52	−5.86
aver abund.	−5.25±0.17		−5.43±0.16		−5.79±0.15		−5.90±0.17	

No Pt II lines were observed. A weak line at 4046.58 Å is Hg I at 4046.56, which is surely not blended with Pt II at 4046.433 Å, because the spectral resolution is high enough, and the rotational velocity is low enough to permit us to see Pt II when it is present. Furthermore, the line observed is reproduced well by assuming the mercury abundance and the isotopic composition deduced from Hg II at 3984 Å (Sect. 3.3).

The comparison with the abundances by Thiam et al. (2010) has shown close agreement between the two determinations. Because Thiam et al. (2010) use an ATLAS9 model computed for solar abundances, the ATLAS12 model computed for an individual abundance may be estimated as unnecessary. However, in addition to the closer values for the Fe I and Fe II abundances obtained with the ATLAS12 model, the consistency of the elemental abundances in the model and in the synthetic spectrum generally gives better agreement between the observed and computed profiles, in particular for the hydrogen profiles when He-weak stars are concerned.

3.2. Emission lines

Emission lines were observed for C I, Ti II, Cr II, Mn II, and possibly for Fe II. Most emissions are so weak that we stated their presence mostly on the basis of the emissions observed in other stars, in particular HD 175640 (Castelli & Hubrig 2004a). The emissions greater than the spectral noise are those listed in Table 2. The atomic data are taken from the Kurucz database[5]. For Mn II mult. 13, only the transition at 6125.861 Å shows true emission, while the other lines at $\lambda\lambda$ 6122.434, 6126.225, 6128.734, 6129.033, 6130.796, and 6131.923 Å are observed to be much weaker than computed, so that we assume that also these Mn II lines are affected by emission.

3.3. Isotopic anomalies

We found an anomalous isotopic composition in HD 71066 for mercury and caicium. Dolk et al. (2003) have determined an anomalous isotopic composition for Hg by analyzing the line of Hg II at 3984 Å. Table 3 shows that our results agree with theirs, while they are somewhat different from those of Thiam et al. (2010). We also obtained very good agreement between the observed and computed line Hg I at 4046.5 Å by adopting the same isotopic composition and abundance (−6.4 dex) derived from Hg II at 3984 Å.

[5] http://kurucz.harvard.edu/atoms.html

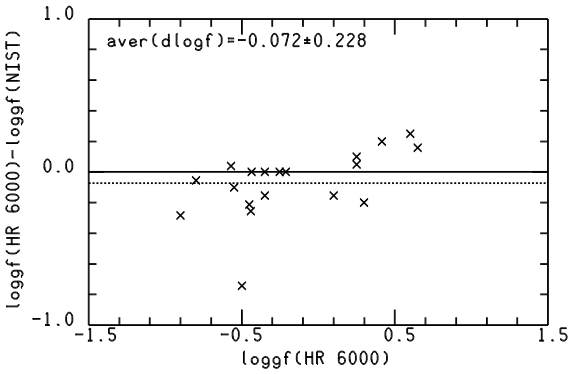

Fig. 1. Comparison of astrophysical log gf-values of Xe II derived from HR 6000 with the log gf-values of the NIST critical compilation.

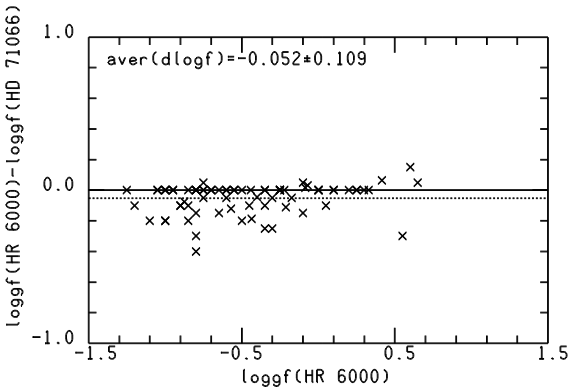

Fig. 2. Comparison of astrophysical log gf-values of Xe II derived from HR 6000 with the astrophysical log gf-values derived from HD 71066.

The lines of the Ca II infrared triplet at $\lambda\lambda$ 8498.023, 8542.091, and 8662.14 Å are redshifted by 0.16 dex. Such a shift, observed in numerous HgMn stars and Ap stars (Cowley et al. 2007) was discovered by Castelli & Hubrig (2004b), who interpret it as due to an anomalous calcium isotopic composition.

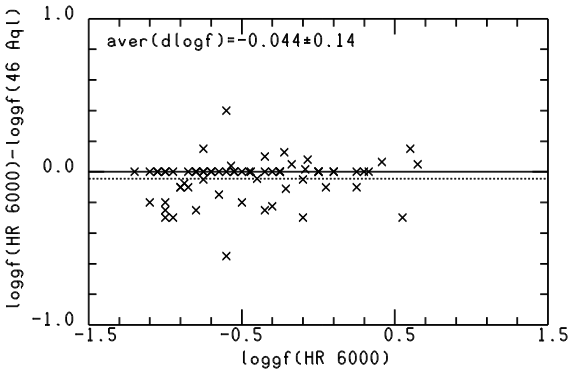

Fig. 3. Comparison of astrophysical log gf-values of Xe II derived from HR 6000 with the astrophysical log gf-values derived from 46 Aql.

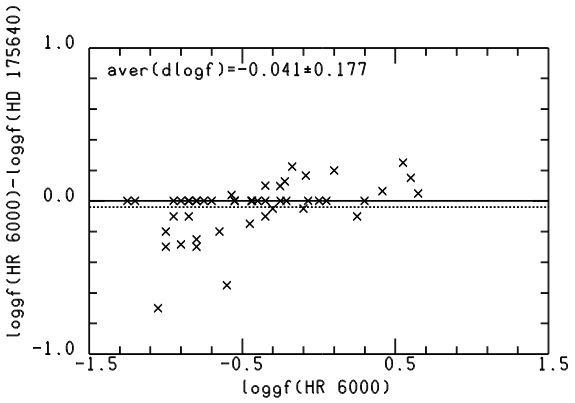

Fig. 4. Comparison of astrophysical log gf-values of Xe II derived from HR 6000 with the astrophysical log gf-values derived from HD 175640.

4. The Xenon abundance in HR 6000, HD 71066, 46 Aql, and HD 175640

To compute the Xe II line spectrum we derived the xenon abundance in each star from the equivalent widths of a set of unblended Xe II lines. The WIDTH code (Kurucz 2005) was used. The selected lines and their atomic data are listed in Table 4. Wavelengths and log gf-values were taken from the NIST database (Version 4)[6]. We assumed the classical radiative damping constant γ_R=0.2223x10$^{16}/\lambda^2$ s^{-1} for λ in Å. For Stark broadening we used the experimental results from Djurovic et al. (2006). Because they are given for a temperature of T=22000 K, we investigated the effect of the temperature on the Stark damping constant γ_S. We interpolated for T=12000 K in the tables from Popovic & Dimitrijevic (1997), which list Stark widths computed at different temperatures. The last two columns of Table 4 compare γ_S values from Djurovic et al. (2006) (Dj) with the interpolated values for temperature from Popovic & Dimitrijevic (1997)(PD). We found that the differences in γ_S from the two sources do not affect the abundances more than 0.01 dex. The approximations of the WIDTH code were used (Castelli 2005) f for no available Stark damping constants and for Van der Waals damping constants.

The measured equivalent widths of the selected Xe II lines and the corresponding abundances are given in Table 5.

5. Stellar wavelengths and the astrophysical log gf-values for Xe II

Because xenon is more abundant in HR 6000 than in the other stars, we searched in the HR 6000 spectra for those Xe II lines with an intensity equal to or higher than 100 in the NIST line list. When these lines were observed in the spectra, they were added in our line list. For lines with no available log gf-values, we assigned guessed values based on the line intensity. We examined the interval 3900-8000 Å with two gaps in the 4525 – 4780 Å and 7536 – 7660 Å regions, due to the lack of spectra in these ranges.

[6] http://www.nist.gov/pml/data/asd.cfm

A synthetic spectrum for HR 6000 was computed for the xenon abundance given in Table 5 and for the abundances of all the other elements as derived by Castelli et al. (2009). In all the stars, the wavelength scale was fixed by shifting the observed spectrum on the computed spectrum until overimposing some lines with well-determined wavelength values such as Ca II 3933.663 Å, Mg II 4481.126 Å, 4481.150 Å, 4481.325 Å, and several strong Fe II lines.

For all the considered Xe II lines, we adjusted the log gf-value until the observed and computed profiles agree best. For several lines we also adjusted the NIST wavelength, because we noticed that, while they do not have an observed counterpart, they are close to an unidentified stellar line with wavelength blueshifted up to 0.1 Å from the predicted Xe II line.

The astrophysical log gf-values and the adjusted wavelengths were then checked on the three other stars by comparing their observed spectra with synthetic spectra computed with the Xe II wavelengths and oscillator strengths obtained from the spectrum of HR 6000. The Xe II abundances adopted for the three stars are those given in Table 5. Table B.1 in Appendix B lists wavelengths and log gf-values as derived from the four stars. We found that for all the examined transitions, the stellar wavelength is the same in the four stars, except for the lines at 5260.44 Å and 6343.96 Å. The largest difference between stellar and NIST wavelength is −0.13 Å observed for the line at 4330.52 Å. This line, as well as all the other lines with $\Delta\lambda\sim-0.1$ Å has a 6d or a 7s level as upper level. The uncertainty of the energy of these levels is on the order of 0.5 cm^{-1} according to Hansen & Persson (1987).

Figures 1, 2, 3, and 4 show the comparison of the HR 6000 astrophysical log gf-values for Xe II with the log gf-values taken from the NIST database and with the the astrophysical log gf-values derived from the spectra of HD 71066, 46 Aql, and HD 175640, respectively (Table B.1, col. 5). The largest discrepancy with the NIST data occurs for the line at 4414.84 Å. We adopted the stellar log gf-value for it because it gives an excellent agreement between the observed and computed profiles in all the four stars we examined. The comparison of the astrophysical log gf-values of HR 6000 with those from the other stars shows that they are on average lower by about 0.04-0.05 dex than those from the other stars and that the mean square deviation from the average increases with the decrease in the xenon abundance. We note that the weaker a line, the more uncertain its astrophysical log gf-value, mostly when the noise is not negligible. In particular, red spectra are affected both by rather large noise and by numerous telluric lines that lower the accuracy of the results.

The final line list for Xe II is shown in Table 6. Columns 1 and 2 give the wavelength derived from the stellar spectra and the astrophysical log gf-value obtained by averaging the astrophysical log gf-values from the four stars. The associated error is the standard deviation from the mean. When it is not given, it means that the log gf-value was obtained from only one star. Columns 3 and 4 list log gf-values from the literature and the source. The literature sources are the NIST database, version 4 (NIST4), and Zíelińska et al. (2002) (ZBD). Zíelińska et al. (2002) estimate that, in general, their experimental transition rates agree with the NIST critical compilation made by Reader et al. (1980), which is the one adopted in the NIST4 database.

The last column gives the γ_{Stark} parameter, which was determined as described in Sect. 4. Figure 5 shows, for each studied star, the comparison of the observed and computed spectra in the region of the Xe II line with wavelength 4462.190 Å, according to the NIST database, and 4462.090 Å, according to Table 6. The wavelength shift of 0.1 Å and the astrophysical log gf value of +0.33, which are the same for all the stars, provide excellent agreement between the observed and computed Xe II profiles.

6. Conclusions

From the high resolution stellar spectra of four HgMn stars we derived both wavelengths and log gf-values for 100 Xe II lines, which should also be observable in the spectra of numerous others chemically peculiar B-type stars. Of these lines, only 22 lines have log gf-values available in the NIST database. The NIST wavelength of two of them, 4180.10 Å and 4330.52 Å, differs by about 0.1 Å from that observed in the spectra. There is a total of 27 lines in our sample for which the observed wavelength differs from the NIST wavelength by more than −0.06 Å with the maximum shift of −0.13 Å for the line at 4330.52 Å. We believe that the wavelength differences are mostly the result of uncorrect energy levels, in that they are all related to 6d or 7s levels, which have an uncertainty of about 0.5 cm^{-1} according to Hansen & Persson (1987). This hypothesis seems us to be more relastic than that of some isotopic anomaly for Xe. For instance, using the isotopic wavelengths from Alvarez et al. (1979), Castelli & Hubrig (2007) excluded that the blueshift of 0.03 Å observed for the Xe II line at 6051.15 Å can be due to some isotopic anomaly. Instead, because no isotopic composition was considered in our computations, owing to the lack of isotopic wavelengths for Xe II, we could explain the larger astrophysical log gf-value than the experimental one obtained for a few lines with the presence of the xenon isotopes, which should not be neglected in the computations of the strongest Xe II line profiles. Good examples are the lines at 4844.33 Å, 5292.22 Å, and 5419.155 Å (Table 6).

On the basis of the wavelength shifts observed in the stellar spectra we redetermined the energy of three 7s, one 5d, and eighteen 6d levels. These levels, together with the old and new energy values, are listed in Table 7. We would like to point out that the new energy values depend, of course, on the accuracy of the energy of the lower level.

The identification of the Xe II lines and their consequent addition in the line lists, increases the accuracy of the synthetic spectra for the CP stars. In fact, it is important to be able to reproduce their high-resolution spectra well, because these stars are an excellent tool for extending laboratory spectrum analyses for several elements. An example is the determination of new high-excitation energy levels for Fe II from the same UVES spectra of HR 6000 used for this paper (Castelli & Kurucz 2010). For instance, As II is another element observed in some CP stars for which not even one log gf-value in the optical region has been found in the literature. As II has not only been observed in 46 Aql (Sadakane et al. 2001, Castelli et al. 2009), but also in HD 71066, as we have shown in this paper. If only one log gf value were given for it, we could derive astrophysical log gf-values for the other lines, just as we did for Xe II.

The abundance analysis of HD 71066 has pointed out the overabundances of Y II, Nd III, Dy III, and Au II for the first time, in addition to the Xe II and As II overabundances. Those of other elements, in particular Hg, P, Ti, Cr, Mn, Fe, and Sr, have already been stated by Thiam et al. (2010) and confirmed by us.

We found that HD 71066 is a typical HgMn star with Hg and Ca isotopic anomalies and emission lines for C I, Ti II, Cr II, and Mn II. He I is underabundant and the shape of its profiles

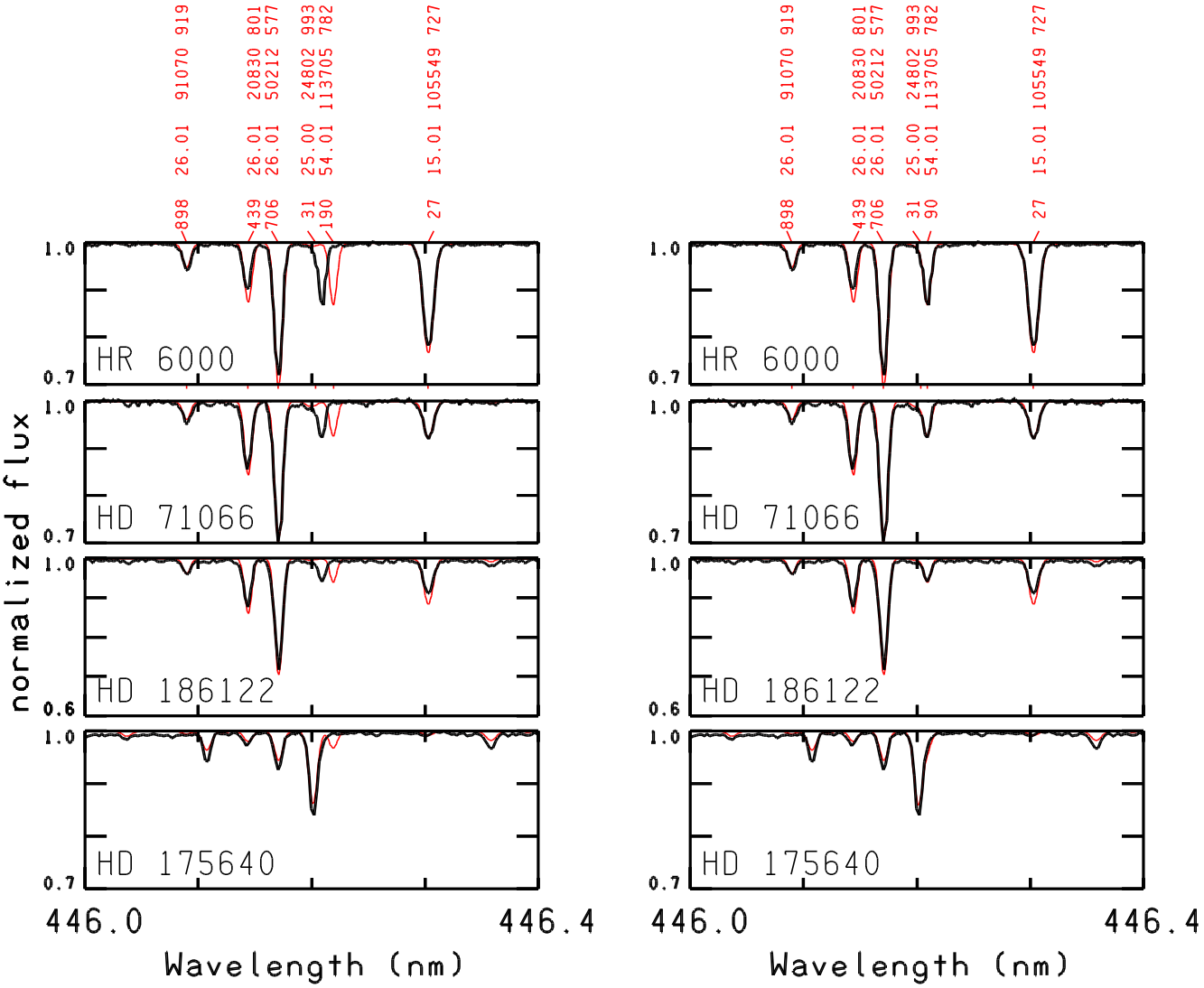

Fig. 5. Comparison for the four stars of the observed (black line) and computed (red line) spectra in the region of the Xe II line with wavelength 446.2190 nm according to the NIST database (left panel) and with wavelength 446.2090 nm according to this paper (right panel). The line identification can be decoded as follows: for the first line, 898 last 3 digits of wavelength 446.0898 nm; 26 atomic number of iron; .01 charge/100; i.e., 26.01 identifies the line as Fe II; 91 070 is the energy of the lower level in cm^{-1}; 919 is the residual central intensity in per mil. The Xe II line is identified by 54.01.

indicates the presence of helium vertical abundance stratification in the atmosphere.

Acknowledgements. Kutluay Yüce was supported by TÜBİTAK (The Scientific and Technological Research Council of Turkey). She thanks TÜBİTAK and Ankara University.

References

Alvarez, E., Arnesen, A., Bengtson, A., Hallin, R., Nordling, C., Noreland, T., Staaf, O., & Mayige, C. 1979, Phys. Scr, 20, 141
Ballester, P., Grosbol, P., Banse, K., et al. 2000, Proc. SPIE, 4010, 246
Biémont, E., Palmeri, P., & Quinet, P. 1999, Ap&SS, 269, 635
Boyce, J. C. 1936, Phys. Rev. 49, 730
Castelli, F. 2005, Memorie della Societa Astronomica Italiana Supplementi, 8, 44
Castelli, F., & Hubrig, S. 2004a, A&A, 425, 263
Castelli, F., & Hubrig, S. 2004b, A&A, 421L, 1
Castelli, F., & Hubrig, S. 2007, A&A, 475, 1041
Castelli, F., Kurucz, R. L., & Hubrig, S. 2009, A&A, 508, 401
Castelli, F., & Kurucz, R. L. 2010, A&A, 520, 57
Cowley, C. R., Hubrig, S., Castelli, F., González, J. F., & Wolff, B. 2007, MNRAS, 377, 1579
Djurovic, S., Pelaez, R. J., Cirisan, M., Aparicio, J. A., & Mar, S. 2006, J. Phys. B: At. Mol. Opt. Phys., 39, 2901
Dolk, L., Wahlgren, G. M., & Hubrig, S. 2003, A&A, 402, 299
Dworetsky, M. M., Persaud, J. L., & Patel, K. 2008, MNRAS, 385, 1523
Fuhr, J. R. & Wiese, W. L., 2006, J. Phys. Chem. Ref. Data, 35, 1669
Gallagher, A. 1967, Phys. Rev. 157, 24
Grevesse, N., & Sauval, A. J. 1998, Space Sci. Rev., 85, 161
Hansen, J. E., & Persson, W. 1987, Phys. Scr., 36, 602
Hauck, B., & Mermilliod, M. 1998, A&AS, 129, 431
Hubrig, S., Castelli, F., & Wahlgren, G. M. 1999, A&A, 346, 139
Hubrig, S., North, P., Schöller, M., & Mathys, G. 2006, Astronomische Nachrichten, 327, 289

Humphreys, C. J. 1939, J. Res. Natl. Bur. Stand. (U.S.), 22, 19
Johansson, S., 2007, private communication
Kurucz, R. L. 1993, SYNTHE Spectrum Synthesis Programs and Line Data, CD-ROM, No. 18
Kurucz, R. L. 2005, Mem. Soc. Astron. Ital. Suppl. 8, 14
Kurucz, R. L., & Peytremann, E. 1975, SAO Special Report, 362
Lanz, T., & Artru, M.-C. 1985, Phys. Scr, 32, 115
Miller, M. H., Roig, R. A., & Bengtson, R. D. 1971, Phys. Rev. A, 4, 1709
Moon, T. T. 1985, Commun. Univ. London. Obs., 78
Nunez, N. E., Gonzalez, J. F., Hubrig, S. 2010, Poster presented at the International Conference "Magnetic Stars", 27 Aug - 1 Sept, 2010, Special Astrophysical Observatory, Zelenchukskaja, Russia
Pickering, J. C., Thorne, A. P., & Perez, R. 2002, ApJS, 138, 247
Popovic, L. C., & Dimitrijevic, M. S. 1996, A&AS, 116, 359
Reader, J., Corliss, C. H., Wiese, W. L., & Martin, G. A. 1980, Wavelengths and transition probabilities for atoms and atomic ions: Part 1. Wavelengths, part 2. Transition probabilities. NSRDS-NBS Vol. 68,
Rosberg, M., & Wyart, J.-F. 1997, Phys. Scr., 55, 690
Sadakane, K., Takada-Hidai, M., Takeda, Y. et al. 2001, PASJ, 53, 1223
Saloman, E. B. 2004, J. Phys. Chem. Ref. Data, 33, 765
Thiam, M., LeBlanc, F., Khalack, V., & Wade, G. A. 2010, MNRAS, 405, 1384
Zielińska, S., Bratasz, Ł., & Dzierżęga, K. 2002, Phys. Scr, 66, 454

Table 6. The final Xe II astrophysical line list for the 3900-4525 Å and 4780-8000 Å intervals. The literature log gf sources are the NIST database, version 4 (NIST4) and Zielińska et al. (2002)(ZBD).

λ	log gf	log gf	source	$log\gamma_S$
stellar	stellar	literature		
3907.820	−0.82±0.06			−4.684
4037.260	−1.00±0.00			
4037.470	−0.75±0.00			
4057.360	−0.80±0.00			−4.899
4157.980	−0.60±0.00			−4.878
4162.160	−1.57±0.03			−5.379
4180.007	−0.35±0.00	−0.35	NIST4	
4193.100	−0.60			
4208.391	−0.38±0.02			
4209.370	−0.70±0.00			
4213.620	−0.22±0.08			
4215.620	−1.05±0.00			
4222.900	+0.64±0.23			−4.778
4238.135	−0.23±0.10			−4.948
4245.300	−0.13±0.07			−4.930
4251.540	−0.58±0.02			−4.722
4296.320	−0.85±0.00			−5.129
4330.390	+0.30±0.00	+0.498	NIST4	−4.884
4369.100	−0.72±0.02			−4.890
4373.700	−0.70±0.00			
4384.910	≤ −1.95			−5.358
4393.090	+0.00±0.00			−4.927
4395.770	+0.00±0.00			−4.884
4414.840	−0.50±0.00	+0.243	NIST4	−5.432
4416.090	−0.80			
4448.025	+0.10±0.05			
4462.090	+0.33±0.00			−4.866
− − − −				
4787.77	−0.82±0.03			−5.324
4817.98	−1.25±0.00			−5.351
4823.25	−0.65±0.00			−4.989
4844.33	+0.61±0.02	+0.491	NIST4	−5.347
		+0.510±0.027	ZBD	
4876.50	+0.10±0.00	+0.255	NIST4	−5.505
4883.53	−0.25±0.00			−5.525
4884.09	−0.80			
4887.30	−0.85±0.05			−5.423
4890.085	−1.17±0.04	−0.754±0.022	ZBD	−5.420
4919.66	−0.85±0.12			
4921.48	+0.05±0.09			−4.442
4971.68	−0.75±0.00			
4972.70	−0.55±0.00			−5.430
4988.725	−0.85±0.09			−5.214

Table 6. cont.

λ	log gf	log gf	source	$log\gamma_S$
stellar	stellar	literature		
5044.92	−0.80±0.00			
5080.51	−0.22±0.12			
5122.31	−0.37±0.09			−4.951
5188.08	−1.10±0.00			
5260.42	−0.37±0.08	−0.437	NIST4	
5261.95	+0.25±0.00	+0.150	NIST4	−5.495
5268.25	−0.80±0.12			−4.978
5292.22	+0.49±0.06	+0.351	NIST4	−5.482
		+0.382±0.013	ZBD	
5309.27	−0.95±0.00			
5313.76	−0.09±0.04			
5339.355	−0.10±0.03	+0.048±0.019	ZBD	
5368.075	−1.05±0.00			
5372.405	−0.15±0.06	−0.211	NIST4	−5.551
5419.155	+0.37±0.03	+0.215	NIST4	−5.481
		+0.256±0.015	ZBD	
5438.96	−0.44±0.00	−0.183	NIST4	−5.544
5450.45	−0.97±0.09			
5460.365	−0.77±0.04	−0.673±0.030	ZBD	−5.531
5472.60	−0.55±0.00	−0.449	NIST4	−5.482
		−0.362±0.030	ZBD	
5531.05	−0.78±0.10	−0.616	NIST4	−5.504
		−0.632±0.021	ZBD	
5616.65	−0.70±0.17			
5659.38	−0.65±0.15			−5.407
5667.540	−0.53±0.08			−5.535
5699.61	−0.85			
5719.587	−0.80±0.00	−0.746	NIST4	
		−0.687±0.023	ZBD	
5726.88	−0.28±0.05			
5750.99	−0.40±0.05			
5758.665	−0.35±0.00			−5.539
5776.39	−0.70			−5.488
5893.29	−0.90			
5905.115	−0.75±0.10			
5945.53	−0.67±0.09			−5.527
5971.135	−0.50			
5976.460	−0.29±0.06	−0.222	NIST4	−5.545
		−0.317±0.023	ZBD	
6036.170	−0.56±0.06	−0.609	NIST4	−5.535
		−0.562±0.020	ZBD	
6051.120	−0.28±0.04	−0.252	NIST4	−5.515
		−0.257±0.020	ZBD	

Table 6. cont.

λ	log gf	log gf	source	$log\gamma_S$
stellar	stellar	literature		
6097.57	−0.39±0.06	−0.237	NIST4	
		−0.355±0.025	ZBD	
6101.37	−0.50±0.28			
6194.07	+0.05±0.15			
6270.81	−0.18±0.12	−0.196	NIST4	−5.510
6277.54	− − −	−0.894	NIST4	−5.543
		−0.778±0.021	ZBD	
6300.830	−1.10			
6343.95	−0.64±0.10	−0.786±0.024	ZBD	
6356.33	−0.25			
6375.28	−1.00			
6512.79	−1.00±0.00			
6528.65	−0.40			
6594.97	0.00±0.00			
6597.23	−0.60±0.00			
6620.02	−0.85±0.00			
6694.285	−0.92±0.12	−0.912±0.020	ZBD	
6788.71	−0.50			
6790.37	−0.70			
6805.74	− − −	−0.595	NIST4	
		−0.547±0.023	ZBD	
6990.835	+0.30±0.05	+0.200	NIST4	
		+0.084±0.032	ZBD	
7082.15	+0.05			
7164.85	+0.20±0.00			
7284.34	−0.50			
7339.30	+0.45?			
7787.04	−0.50?			

Table 7. A few 7s, 5d, and 6d even Xe II energy levels from Hansen & Persson (1987) modified according to the wavelength positions observed in the UVES spectra of HR 6000, HD 71066, 46 Aql, and HD 175640

Term		level value (cm^{-1})	
		NIST	This paper
$5s^25p^4(^3P_2)7s$	$[2]_{5/2}$	132518.82	132519.23
	$[2]_{3/2}$	133189.42	133189.94
$5s^25p^4(^3P_0)7s$	$[0]_{1/2}$	140883.42	140883.79
$5s^25p^4(^1D_2)5d$	$[0]_{1/2}$	135060.97	135061.36
$5s^25p^4(^3P_2)6d$	$[4]_{9/2}$	136109.65	136110.13
	$[4]_{7/2}$	136597.81	136598.48
	$[3]_{7/2}$	135507.32	135507.72
	$[3]_{5/2}$	139094.28	139094.83
	$[2]_{5/2}$	135547.13	135547.53
	$[2]_{3/2}$	135708.32	135708.72
	$[1]_{3/2}$	139640.43	139640.61
	$[1]_{1/2}$	136554.11	136554.47
$5s^25p^4(^3P_1)6d$	$[3]_{7/2}$	145587.61	145588.12
	$[3]_{5/2}$	146927.86	146928.34
	$[2]_{3/2}$	145940.34	145940.79
	$[1]_{3/2}$	148085.19	148085.36
	$[1]_{1/2}$	145222.72	145223.16
$5s^25p^4(^3P_0)6d$	$[2]_{5/2}$	144384.90	144385.45
	$[2]_{3/2}$	144140.16	144140.69
$5s^25p^4(^1D_2)6d$	$[4]_{9/2}$	152806.73	152806.73 ?
	$[4]_{7/2}$	152708.92	152709.19
	$[1]_{3/2}$	153584.09	153584.02

Appendix A: The lines used for the abundance analysis of HD 71066

Table A.1 lists the lines that were used to derive the abundances of HD 71066. The wording "not obs" is given for lines not present in the spectra, while the wordings "profile" and "blend" are given for lines observed well in the spectra, but that do not have measurable equivalent widths either because the noise affects the profile too much or because other components affect the line. These wordings also indicate lines for which adequate equivalent widths cannot be computed, as in the cases of Mg II at 4481 Å which is a blend of transitions belonging to the same multiplet, of most Mn II lines that are affected by hyperfine structure, of the Ca II infrared triplet, which is a blend of isotopic components, and so on. For the remaining lines the measured equivelent widths are given in the table.

Appendix B: The investigated Xe II lines in HR 6000, HD 71066, 46 Aql, and HD 175640

Table B.1 gives the details on the determination of the Xe II wavelengths and log gf-values from the spectra of the four stars. It lists in successive columns the laboratory wavelengths and the line intensity taken from the NIST database (footnote 6), the stellar wavelengths as derived from HR 6000, HD 71066, 46 Aql, and HD 175640. If the observed wavelength is the same in all the stars, only that of HR 6000 is given. HR 6000, HD 71066, 46 Aql, and HD 175640 are indicated in col. 6 with the numbers 1,2, 3, and 4, respectively. A question mark means uncertain determinations from that star. The wavelength difference $\Delta\lambda$=λ(stellar)-λ(lab) is given in col. 4. The energy and the configuration of the lower and upper level of the transition are given in cols. 7,8,9, and 10, respectively. The last column adds some notes about the observed lines. Table B.1 lists also the NIST log gf-values and the log gf-values derived from the experimental transition rates determined by Zíelińska et al. (2002).

Table A.1. Abundances of HD 71066 from the ATLAS12 model with parameters $T_{\rm eff}$=12000 K, log g=4.1

				HD 71066[12000,4.1,AT12]			
Species	λ(Å)	log gf	Ref.[a]	χ_{low}	W(mÅ)	$log(N_Z)/N_{\rm tot})$	Notes
He I[a]	4026.209	−0.374	NIST4	169087.008	profile	−2.28	the core is computed too strong
He I	4471.502	+0.043	NIST4	169087.008	profile	−2.28	the core is computed too strong
He I	5875.661	+0.739	NIST4	169086.964	profile	−2.50	the core is computed too strong
He I	6678.151	+0.328	NIST4	171135.00	profile	−2.50	
Be II	3130.420	−0.178	NIST4	0.00	profile	−10.80	
C II	3918.968	−0.533	NIST4	131724.370	profile	−3.90	observed at 3918.92
C II	4267.001	+0.563	NIST4	145549.270	profile	−3.90	observed at 4267.10
C II	4267.261	+0.716	NIST4	145550.700	profile	−3.90	
C II	4267.261	−0.584	NIST4	145550.700	profile	−3.90	
C II	6578.052	−0.021	NIST4	116537.65	profile	−3.90	
C II	7236.420	+0.294	NIST4	131735.52	profile	−3.90	observed at 7236.35
N I	8680.282	+0.359	NIST4	83364.620	not obs	≤−5.50	
N I	8683.403	+0.105	NIST4	88317.830	not obs	≤−5.50	
O I	4368.193	−2.665	NIST4	76794.978	profile	−3.70	
O I	4368.242	−1.964	NIST4	76794.978	profile	−3.70	
O I	4368.258	−2.186	NIST4	76794.978	profile	−3.70	
O I	5329.096	−1.938	NIST4	86625.757	profile	−3.67:	
O I	5329.099	−1.586	NIST4	86625.757	profile	−3.67:	
O I	5329.107	−1.695	NIST4	86625.757	profile	−3.67:	
O I	6155.961	−1.363	NIST4	86625.757	profile	−3.57	
O I	6155.971	−1.011	NIST4	86625.757	profile	−3.57	
O I	6155.989	−1.120	NIST4	86625.757	profile	−3.57	
O I	6156.737	−1.487	NIST4	86627.778	profile	−3.57	
O I	6156.755	−0.898	NIST4	86627.778	profile	−3.57	
O I	6156.778	−0.694	NIST4	86627.778	profile	−3.57	
O I	6454.444	−1.066	NIST4	86627.778	profile	−3.57	
O I	6455.977	−0.920	NIST4	86631.454	profile	−3.60	
O I	7002.173	−2.644	NIST4	88631.146	profile	−3.58	
O I	7002.196	−1.489	NIST4	88631.146	profile	−3.58	
O I	7002.230	−0.741	NIST4	88631.146	profile	−3.58	
O I	7002.250	−1.364	NIST4	88631.303	profile	−3.58	
Ne I	6402.248	+0.345	NIST4	134041.840	not obs	≤−5.70	
Ne I	7032.413	−0.249	NIST4	134041.840	not obs	≤−5.70	
Na I	5889.950	+0.108	NIST4	0.00	38.2	−5.42	
Na I	5895.924	−0.194	NIST4	0.00	19.3	−5.62	

Table A.1. cont.

					HD 71066[12000,4.1,AT12]		
Species	λ(Å)	log gf	Ref.[a]	χ_{low}	W(mÅ)	$log(N_Z)/N_{tot})$	Notes
Mg I	5167.321	−0.870	NIST4	21850.405	1.30	−5.36	
Mg I	5172.684	−0.393	NIST4	21870.464	4.60	−5.27	
Mg II	4481.126	+0.749	NIST4	71490.190	profile	−5.40	
Mg II	4481.150	−0.553	NIST4	71490.190	profile	−5.40	
Mg II	4481.325	+0.594	NIST4	71491.063	profile	−5.40	
Al I	3944.006	−0.638	NIST4	0.000	not obs	≤−7.30	
Al I	3961.520	−0.336	NIST4	112.061	not obs	≤−7.30	
Al II	7056.712	+0.110	NIST4	91274.500	not obs	≤−7.30	
Si II	3853.665	−1.341	NIST4	55309.350	66.7	−4.81	
Si II	3856.018	−0.406	NIST4	55325.180	113.7	−4.91	
Si II	3862.595	−0.757	NIST4	55309.350	101.4	−4.74	
Si II	4072.709	−2.701	NIST4	79338.500	2.3	−4.32	
Si II	4075.452	−1.400	NIST4	79355.020	16.37	−4.65	
Si II	4190.724	−0.351	LA	108820.600	8.35	−4.58	
Si II	4198.133	−0.611	LA	108778.700	5.98	−4.48	
Si II	5041.024	+0.029	NIST4	81191.340	82.89	−4.35	
Si II	5055.984	+0.523	NIST4	81251.320	100.6	−4.60	
Si II	5056.317	−0.492	NIST4	81251.320	46.08	−4.48	
Si II	5957.559	−0.225	NIST4	81191.340	44.44	−4.57	
Si II	5978.930	+0.084	NIST4	81251.320	56.53	−4.62	
Si II	7849.722	+0.470	NIST4	101024.350	10.65	−4.94	
P II	4044.576	+0.481	K,MRB	107360.250	18.35	−5.04	
P II	4127.559	−0.110	K,KP	103667.860	8.01	−5.13	
P II	4288.606	−0.630	K,MRB	101635.690	2.10	−5.34	
P II	4420.712	−0.329	NIST4	88893.220	15.97	−5.12	
P II	4452.472	−0.194	K,MRB	105302.170	6.30	−5.00	
P II	4463.027	+0.026	K,MRB	105549.670	8.67	−5.04	
P II	4466.140	−0.560	NIST4	105549.670	1.83	−5.24	
P II	4475.270	+0.440	NIST4	105549.670	13.15	−5.20	
P II	5296.077	−0.160	NIST4	87124.600	22.90	−4.86	
P II	5344.729	−0.390	NIST4	86597.550	15.49	−4.99	
P II	5425.880	+0.180	NIST4	87124.600	31.31	−4.92	
P II	6034.039	−0.220	NIST4	86597.550	16.81	−4.95	
P II	6043.084	+0.416	NIST4	87124.600	32.87	−4.94	

Table A.1. cont.

					HD 71066[12000,4.1,AT12]		
Species	λ(Å)	log gf	Ref.[a]	χ_{low}	W(mÅ)	$log(N_Z)/N_{tot})$	Notes
P III	4222.198	+0.210	NIST4	117835.950	4.99	−5.13	
S II	4153.068	+0.617	NIST4	128233.200	2.98	−5.66	
S II	4162.665	+0.777	NIST4	128599.160	2.67	−5.87	
Ca I	4226.728	+0.244	NIST4	0.000	profile	−5.68	
Ca II	3158.869	+0.27	NIST4	25191.51	29.96	−6.60	
Ca II	3179.331	+0.52	NIST4	25414.40	32.47	−6.73	
Ca II	3181.275	−0.45	NIST4	25414.40	15.90	−6.45	
Ca II	3933.663	+0.135	NIST4	0.000	profile	−6.33	
Ca II	3968.469	−0.18	NIST4	0.000	profile	−6.90	
Ca II	8498.023	−1.45	GAL	13650.19	profile	−6.33	$\Delta\lambda$=+0.16
Ca II	8542.091	−0.50	GAL	13710.88	profile	−6.33	$\Delta\lambda$=+0.16
Ca II	8662.142	−0.76	GAL	13650.19	profile	−6.33	$\Delta\lambda$=+0.16
Sc II	4246.822	+0.242	NIST4	2540.950	not obs	≤−10.5	
Sc II	4314.083	−0.100	NIST4	4987.790	not obs	≤−10.5	
Ti II	4163.644	−0.130	PTP	20891.660	40.17	−6.45	
Ti II	4287.873	−1.790	PTP	8710.440	9.09	−6.51	
Ti II	4290.215	−0.850	PTP	9395.710	37.88	−6.51	
Ti II	4294.094	−0.930	PTP	9744.250	40.01	−6.41	
Ti II	4300.042	−0.440	PTP	9518.060	57.29	−6.39	
Ti II	4301.922	−1.150	PTP	9363.620	24.83	−6.55	
Ti II	4367.652	−0.860	PTP	20891.660	12.52	−6.53	
Ti II	4395.031	−0.540	PTP	8744.250	55.79	−6.38	
Ti II	4399.765	−1.190	PTP	9975.920	24.64	−6.94	
Ti II	4411.072	−0.670	PTP	24961.030	13.25	−6.48	
Ti II	4417.714	−1.190	PTP	9395.710	24.69	−6.44	
Ti II	4443.810	−0.720	PTP	8710.440	49.85	−6.37	
Ti II	4464.448	−1.810	PTP	9363.620	9.85	−6.42	
Ti II	4468.492	−0.620	NIST4	9118.260	51.86	−6.41	
Ti II	4488.325	−0.510	PTP	25192.710	16.92	−6.46	
Ti II	4805.085	−1.120	NIST4	16625.110	18.79	−6.31	
Ti II	4911.195	−0.610	PTP	25192.790	14.40	−6.44	
V II	3093.105	+0.559	K10V	3162.800	not obs	≤−10.0	
V II	3102.294	+0.434	K10V	2968.220	not obs	≤−10.0	

Table A.1. cont.

					HD 71066[12000,4.1,AT12]		
Species	λ(Å)	log gf	Ref.[a]	χ_{low}	W(mÅ)	$log(N_Z)/N_{tot}$)	Notes
Cr II	4812.337	−1.997	K10Cr	31168.580	6.07	−6.22	
Cr II	4824.127	−0.980	K10Cr	31219.350	39.36	−6.06	
Cr II	4836.229	−1.963	K10Cr	31117.390	7.39	−6.16	
Cr II	5237.329	−1.160	NIST4	32854.310	22.48	−6.24	
Cr II	5246.768	−2.460	NIST4	29951.880	2.93	−6.17	
Mn II	3917.318	−1.135	K09Mn	55759.270	profile	−5.93	
Mn II	4363.255[b]	−1.887	K09Mn	44899.820	profile	−5.93	
Mn II	4365.217[b]	−1.344	K09Mn	44899.820	profile	−5.93	
Mn II	4478.637[b]	−0.945	K09Mn	53597.130	profile	−5.93	
Mn II	4806.823	−1.571	K09Mn	43696.120	profile	−6.03	
Fe I	3581.193	+0.406	FW06	6928.27	28.28	−3.68	
Fe I	3618.768	−0.003	FW06	7985.78	15.49	−3.88	
Fe I	4005.242	−0.610	FW06	12560.93	14.40	−3.87	
Fe I	4071.738	−0.022	FW06	12698.55	31.00	−3.91	
Fe I	4202.029	−0.708	FW06	11976.24	13.44	−3.85	
Fe I	4219.360	+0.000	FW06	28819.95	7.80	−3.82	
Fe I	4235.936	−0.341	FW06	19562.44	12.27	−3.81	
Fe I	4271.760	−0.164	FW06	11976.24	30.68	−3.84	
Fe I	4383.545	+0.200	FW06	11976.24	43.10	−3.85	
Fe I	4404.750	−0.142	FW06	12560.93	29.22	−3.87	
Fe I	4415.122	−0.615	FW06	12968.55	14.49	−3.84	
Fe I	5364.871	+0.228	FW06	35856.40	3.77	−3.96	
Fe II	4128.748	−3.580	FW06	20830.58	31.85	−3.92	
Fe II	4178.862	−2.440	FW06	20830.58	67.36	−3.96	
Fe II	4273.326	−3.300	FW06	21812.05	41.90	−3.86	
Fe II	4296.572	−2.930	FW06	21812.05	54.16	−3.85	
Fe II	4369.411	−3.580	FW06	22409.85	27.75	−3.93	
Fe II	4413.601	−4.190	FW06	21581.64	15.83	−3.75	
Fe II	4416.830	−2.600	FW06	22409.85	64.47	−3.83	
Fe II	4491.405	−2.640	FW06	23031.30	57.57	−3.96	
Fe II	4508.288	−2.350	FW06	23031.30	73.82	−3.76	
Fe II	4515.339	−2.360	FW06	23939.36	65.01	−3.94	
Fe II	4913.295	+0.016	J07	82978.71	33.22	−3.77	
Fe II	4993.358	−3.680	FW06	22637.20	26.98	−3.83	
Fe II	5001.953	+0.933	J07	82853.65	65.38	−3.85	
Fe II	5030.631	+0.431	FW06	82978.68	44.23	−3.87	
Fe II	5035.700	+0.630	FW06	82978.68	52.34	−3.84	

Table A.1. cont.

					HD 71066[12000,4.1,AT12]		
Species	λ(Å)	log gf	Ref.[a]	χ_{low}	W(mÅ)	$log(N_Z)/N_{tot})$	Notes
Fe II	5144.352	+0.307	FW06	84424.37	23.98	−4.24	
Fe II	5247.956	+0.550	FW06	84938.18	41.29	−3.88	
Fe II	5260.254	+1.090	J07	84863.38	65.44	−3.84	
Fe II	5276.002	−1.900	FW06	25805.33	76.52	−3.95	
Fe II	5339.592	+0.568	J07	84296.87	44.50	−3.85	
Fe II	5414.852	−0.258	J07	84863.38	20.80	−3.72	
Fe II	5425.257	−3.390	FW06	25805.33	36.19	−3.64	
Fe II	5465.932	+0.348	FW06	85679.70	38.16	−3.70	
Fe II	5493.830	+0.259	FW06	84685.20	33.73	−3.80	
Fe II	5506.199	+0.923	J07	84863.38	53.95	−3.89	
Fe II	5510.783	+0.043	J07	85184.77	27.35	−3.76	
Co II	4160.657	−1.751	K06Co	27484.371	blend	≤−7.88	
Ni II	4067.031	−1.834	K03Ni	32499.530	blend	≤−7.90	
Cu II	4909.734	+0.790	K03Cu	115568.985	not obs	≤−7.8	
Zn II	4911.625	+0.540	NIST4	96909.740	not obs	≤−7.94	
As II	4466.348						
As II	4494.230						
As II	5105.58			81508.925	3.74		
As II	5231.38			79128.330	3.16		
As II	5331.23			81508.925	7.07		
As II	5497.727			78730.893	4.52		blend
As II	5558.09			79128.330	7.11		blend
As II	5651.32			81508.925	9.29		
As II	6110.07			82819.214	2.32		
As II	6170.27			79128.330	2.62		blend
Sr II	4077.709	+0.151	NIST4	0.000	32.45	−8.27	
Y II	3950.349	−0.485	NIST4	840.213	17.38	−7.68	
Y II	4883.682	+0.070	NIST4	8743.316	25.22	−7.49	
Y II	4900.120	−0.090	NIST4	8328.041	20.57	−7.52	

Table A.1. cont.

					HD 71066[12000,4.1,AT12]		
Species	λ(Å)	log gf	Ref.[a]	χ_{low}	W(mÅ)	$log(N_Z)/N_{tot})$	Notes
Xe II	4844.33	+0.49	NIST4	93068.440	20.72	−5.43	
Xe II	5292.21	+0.35	NIST4	93068.440	19.72	−5.20	
Xe II	5419.14	+0.21	NIST4	95064.38	14.27	−5.24	
Xe II	5438.97	−0.19	NIST4	102799.07	2.93	−5.55	
Xe II	5472.61	−0.45	NIST4	95437.67	5.03	−5.34	
Xe II	5531.06	−0.62	NIST4	95437.67	1.87	−5.71	
Xe II	5719.61	−0.74	NIST4	96033.48	1.40	−5.64	
Xe II	5976.46	−0.22	NIST4	95064.38	4.70	−5.49	
Xe II	6036.20	−0.61	NIST4	95396.74	2.44	−5.45	
Xe II	6051.15	−0.25	NIST4	95437.67	4.59	−5.44	
Xe II	6097.59	−0.24	NIST4	95436.74	3.93	−5.53	
Xe II	6990.88	+0.20	NIST4	99409.99	5.18	−5.36	
Nd III	4927.488	−0.83	DREAM	3715.	1.78	−9.63	
Nd III	5294.113	−0.65	DREAM	0.	4.12	−9.62	
Dy III	3930.640	−0.88	DREAM	0.	profile	−9.90	
Au II	4016.067	−1.88	RW	84510.894	2.39	−7.15	
Au II	4052.790	−1.69	RW	84510.894	3.99	−7.08	
Hg I	4358.314	−0.321	NIST4	39412.300	profile	−6.40	
Hg II	3983.890	−1.51	NIST4	35514.000	profile	−6.40	
Hg II	5677.102	+0.82	NIST4	105543.000	5.56	−6.19	blend

[a] He I profiles were compute as described in Castelli & Hubrig (2004a). The wavelengths and log gf-values are multiplet values.
[b] The hyperfine structure was considered in the line profile computations.
DREAM: Biémont et al.(1999): http://w3.umons.ac.be/~astro/dream.shtml;
NIST4: NIST Atomic Spectra Database, version 4 at http://physics.nist.gov/pml/data/asd.cfm;
FW06: Fuhr & Wiese (2006); GAL: Gallagher (1967); LA: Lanz & Artru (1985); PTP: Pickering et al. (2002);
J07: Johansson (2007);
K03Ni: http://kurucz.harvard.edu/atoms/2801/gf2801.pos;
K03Cu: http://kurucz.harvard.edu/atoms/2901/gf2901.pos;
K06Co: http://kurucz.harvard.edu/atoms/2701/gf2701.pos;
K09Mn: http://kurucz.harvard.edu/atoms/2501/gf2501.pos;
K10V: http://kurucz.harvard.edu/atoms/2301/gf2301.pos;
K10Cr: http://kurucz.harvard.edu/atoms/2401/gf2401.pos;
"K" before another log gf source means that the log gf is from the Kurucz files available at http://kurucz.harvard.edu/linelists/gf100/; in particular:
KP: Kurucz & Peytremann (1975); MRB: Miller et al. (1971);
RW: Rosberg & Wyart (1997).

Table B.1. Xe II lines examined in HR 6000, HD 71066, 46 Aql, and HD 175640. The stars are indicated in col. 6 with the numbers 1,2,3, and 4, respectively. The "N" in column 5 indicates that the log gf-value was taken from the NIST database, while "ZBD" indicates data from Zíelińska et al. (2002)

λ(Lab)	Int.	λ(stellar)	$\Delta\lambda$	log gf		χ_{low}(cm^{-1})	Term		χ_{up}(cm^{-1})	Term		Notes
3907.91	100	3907.820	−0.09	−0.75	1	113512.36	$(^3P_2)6p$	$[3]_{5/2}$	139094.28	$(^3P_2)6d$	$[3]_{5/2}$	
				−0.80	2							blend
				−0.90	3							blend
4037.29	100	4037.260	−0.03	−1.00	1,2,3	111792.17	$(^3P_2)6p$	$[2]_{3/2}$	136554.11	$(^3P_2)6d$	$[1]_{1/2}$	broad weak blend
4037.59	200	4037.470	−0.12	−0.75	1,2,3	121179.80	$(^3P_1)6p$	$[0]_{1/2}$	145940.34	$(^3P_1)6d$	$[2]_{3/2}$	broad weak blend
4057.46	200	4057.360	−0.10	−0.80:	1,2?,3	111958.89	$(^3P_2)6p$	$[2]_{5/2}$	136597.81	$(^3P_2)6d$	$[4]_{7/2}$	blend
4158.04	200	4157.980	−0.06	−0.60	1,2?,3	121179.80	$(^3P_1)6p$	$[0]_{1/2}$	145222.72	$(^3P_1)6d$	$[1]_{1/2}$	blend
4162.16	60	4162.160	+0.00	−1.60	1	107904.50	$(^3P_1)5d$	$[1]_{3/2}$	131923.79	$(^1D_2)6p$	$[2]_{3/2}$	blend,weak,3 noise
				−1.55	2							
4180.10	1000	4180.007	−0.093	−0.35N	1,2,3	129667.35	$(^1D_2)6p$	$[1]_{3/2}$	153584.09	$(^1D_2)6d$	$[1]_{3/2}$	blend
4193.15	500	4193.100	−0.05	−0.60	1	128867.20	$(^1D_2)6p$	$[3]_{5/2}$	152708.92	$(^1D_2)6d$	$[4]_{7/2}$	
4208.48	400	4208.391	−0.089	−0.40	1,4	111792.17	$(^3P_2)6p$	$[2]_{3/2}$	135547.13	$(^3P_2)6d$	$[2]_{5/2}$	
				−0.36	2,3							
4209.47	200	4209.370	−0.10	−0.70	1,2,3,4?	111958.89	$(^3P_2)6p$	$[2]_{5/2}$	135708.32	$(^3P_2)6d$	$[2]_{3/2}$	4 blend
4213.72	400	4213.620	−0.10	−0.30	1	120414.87	$(^3P_0)6p$	$[1]_{1/2}$	144140.16	$(^3P_0)6d$	$[2]_{3/2}$	blend
				−0.25	2,4							
				−0.08	3							
4215.60	200	4215.620	+0.02	−1.05	1,2,3	93068.44	$(^3P_2)6s$	$[2]_{5/2}$	116783.09	$(^3P_2)6p$	$[1]_{3/2}$	blend
4223.00	400	4222.900	−0.10	+0.55	1	123254.60	$(^3P_1)6p$	$[2]_{3/2}$	146927.86	$(^3P_1)6d$	$[3]_{5/2}$	
				+0.85	2,3							
				+0.30	4							
4238.25	500	4238.135	−0.115	−0.18	1	111958.89	$(^3P_2)6p$	$[2]_{5/2}$	135547.13	$(^3P_2)6d$	$[2]_{5/2}$	
				−0.13	2							
				−0.23	3							
				−0.40	4							
4245.38	500	4245.300	−0.08	−0.08	1	111958.89	$(^3P_2)6p$	$[2]_{5/2}$	135507.32	$(^3P_2)6d$	$[3]_{7/2}$	
				−0.10	2,3							
				−0.25	4							
4251.57	100	4251.540	−0.03	−0.60	1?	124571.09	$(^3P_1)6p$	$[1]_{1/2}$	148085.19	$(^3P_1)6d$	$[1]_{3/2}$	blend
				−0.55	2?							blend
4296.40	500	4296.320	−0.08	−0.85	1,2,3,4	111792.17	$(^3P_2)6p$	$[2]_{3/2}$	135060.97	$(^1D_2)5d$	$[0]_{1/2}$	
4330.52	1000	4330.390	−0.13	+0.30	1,2,3,4	113512.36	$(^3P_2)6p$	$[3]_{5/2}$	136597.81	$(^3P_2)6d$	$[4]_{7/2}$	
				+0.498N								
4369.20	200	4369.100	−0.10	−0.75	1	113672.89	$(^3P_2)6p$	$[1]_{1/2}$	136554.11	$(^3P_2)6d$	$[1]_{1/2}$	
				−0.70	2?,3							2 blend
4373.78	100	4373.700	−0.08	−0.70	1,2?,3?	116783.09	$(^3P_2)6p$	$[1]_{3/2}$	139640.43	$(^3P_2)6d$	$[1]_{3/2}$	blend
4384.93	60	4384.91	−0.02	−1.95	1,3	90873.83	$5s5p^6$	$^2S_{1/2}$	113672.89	$(^3P_2)6p$	$[1]_{1/2}$	blend
				≤ -2.50	2							not observed
4393.20	500	4393.090	−0.11	+0.00	1,2,3,4?	121628.82	$(^3P_0)6p$	$[1]_{3/2}$	144384.90	$(^3P_0)6d$	$[2]_{5/2}$	
4395.77	500	4395.770 :	0.00	+0.00	1?,2?,3?	130063.96	$(^1D_2)6p$	$[3]_{7/2}$	152806.73	$(^1D_2)6d$	$[4]_{9/2}$	blend

Table B.1. cont.

λ(Lab)	Int.	λ(stellar)	$\Delta\lambda$	log gf		χ_{low}(cm^{-1})	Term		χ_{up}(cm^{-1})	Term		Notes
4414.84	300	4414.84	0.00	−0.50	1,2,3	109563.14	(^{1}D$_2$)6p	[3]$_{7/2}$	132207.76	(^{1}D$_2$)6p	[2]$_{5/2}$	2,4 blend
				+0.243N								
4416.07	150	4416.090	+0.02	−0.80	1 ?	124289.45	(^{3}P$_1$)6p	[1]$_{3/2}$	146927.86	(^{3}P$_1$)6d	[3]$_{5/2}$	3 noise
4448.13	500	4448.025	−0.105	+0.05	1,4	123112.54	(^{3}P$_1$)6p	[2]$_{5/2}$	145587.61	(^{3}P$_1$)6d	[3]$_{7/2}$	
				+0.15	2,3							
4462.19	1000	4462.090	−0.10	+0.33	1,2,3	113705.40	(^{3}P$_2$)6p	[3]$_{7/2}$	136109.65	(^{3}P$_2$)6d	[4]$_{9/2}$	4 blend
− − −−												
4787.77	100	4787.77	0.00	−0.88	1	111326.96	(^{3}P$_1$)5d	[2]$_{3/2}$	132207.76	(^{1}D$_2$)6p	[2]$_{5/2}$	noise?
				−0.80	2,3							
4818.02	200	4817.98	−0.04	−1.25	1,2,4	96033.48	(^{3}P$_2$)5d	[2]$_{3/2}$	116783.09	(^{3}P$_2$)6p	[1]$_{3/2}$	3 artifact
4823.35	300	4823.25	−0.10	−0.65	1,2,3	111792.17	(^{3}P$_2$)6p	[2]$_{3/2}$	132518.82	(^{3}P$_2$)7s	[2]$_{5/2}$	4 blend
4844.33	2000	4844.33	0.00	+ 0.65	1	93068.44	(^{3}P$_2$)6s	[2]$_{5/2}$	113705.40	(^{3}P$_2$)6p	[3]$_{7/2}$	
				+0.60	2,3,4							
				+0.491N								
				+0.510±0.027ZBD								
4876.50	500	4876.50	0.00	+0.10	1,2,3	109563.14	(^{1}D$_2$)6s	[2]$_{5/2}$	130063.96	(^{1}D$_2$)6p	[3]$_{7/2}$	4 blend
				+0.255N								
4883.53	600	4883.53	0.00	−0.25	1,2,3	101157.48	(^{3}P$_0$)6s	[0]$_{1/2}$	121628.82	(^{3}P$_0$)6p	[1]$_{3/2}$	
4884.15	100	4884.09	−0.06	−0.80	1	120414.87	(^{3}P$_0$)6p	[1]$_{1/2}$	140883.42	(^{3}P$_0$)7s	[0]$_{1/2}$	2,3,4 not obs.
4887.30	300	4887.30	0.00	−0.90	1,4	102799.07	(^{3}P$_1$)6s	[1]$_{3/2}$	123254.60	(^{3}P$_1$)6p	[2]$_{3/2}$	
				−0.80	2,3							
4890.090	300	4890.085	−0.005	−1.20	1,3,4	93068.44	(^{3}P$_2$)6s	[2]$_{5/2}$	113513.36	(^{3}P$_2$)6p	[3]$_{5/2}$	
				−1.10	2							
				−0.754±0.022ZBD								
4919.66	200	4919.66	0.00	−0.95	1,2	04250.06	(^{3}P$_1$)5d	[1]$_{1/2}$	124571.09	(^{3}P$_1$)6p	[1]$_{1/2}$	
				−0.65	3							
				−0.85	4							
4921.48	800	4921.48	0.00	+ 0.10	1,2,3	102799.07	(^{3}P$_1$)6s	[1]$_{3/2}$	123112.54	(^{3}P$_1$)6p	[2]$_{5/2}$	
				−0.10	4							
4971.71	200	4971.68	−0.03	−0.75	1,2,3,4	119085.49.	(^{1}D$_2$)5d	[3]$_{5/2}$	139193.80	(^{3}P$_2$)7p	[1]$_{3/2}$	2,3,4 noise
4972.71	400	4972.70	−0.01	−0.55	1,2,3,4	109563.14	(^{1}D$_2$)6s	[2]$_{5/2}$	129667.35	(^{1}D$_2$)6p	[1]$_{3/2}$	
4988.77	300	4988.725	−0.045	−1.00	1	104250.06	(^{3}P$_1$)5d	[1]$_{1/2}$	124289.45	(^{3}P$_1$)6p	[1]$_{3/2}$	blend
				−0.80	2,3,4							
5044.92	150	5044.92	0.00	−0.80	1,2,4	112924.84	(^{1}D$_2$)6s	[2]$_{3/2}$	132741.15	(^{1}D$_2$)6p	[1]$_{1/2}$	3,4 noise
5080.62	600	5080.51	−0.11	−0.30	1,3	113512.36	(^{3}P$_2$)6p	[3]$_{5/2}$	133189.42	(^{3}P$_2$)7s	[2]$_{3/2}$	
				−0.05	2							
5122.42	200	5122.31	−0.11	−0.50	1	113672.89	(^{3}P$_2$)6p	[1]$_{1/2}$	133189.42	(^{3}P$_2$)7s	[2]$_{3/2}$	4 noise
				−0.30	2,3							3 blend
5188.04	200	5188.08	+0.04	−1.10	1,3	123112.54	(^{3}P$_1$)6p	[2]$_{5/2}$	142382.13	(^{3}P$_1$)7s	[1]$_{3/2}$	2 blend, 4 not obs

Table B.1. cont.

λ(Lab)	Int.	λ(stellar)	$\Delta\lambda$	log gf		χ_{low}(cm^{-1})	Term		χ_{up}(cm^{-1})	Term		Notes
5260.44	200	5260.42	−0.02	−0.437N	1,4	104250.06	(^{3}P$_1$)5d	[1]$_{1/2}$	123254.60	(^{3}P$_1$)6p	[2]$_{3/2}$	
				−0.25	2							
		5260.44	0.00	−0.35	3							
5261.95	200	5261.95	0.00	+0.25	1,2,3	112924.84	(^{1}D$_2$)6s	[2]$_{3/2}$	131923.79	(^{1}D$_2$)6p	[2]$_{3/2}$	
				+0.150N								
5268.31	50	5268.25	−0.06	−1.00	1	105313.33	(^{3}P$_2$)5d	[1]$_{3/2}$	124289.45	(^{3}P$_1$)6p	[1]$_{3/2}$	
				−0.80	2							
				−0.70	3,4							
5292.22	1000	5292.22	0.00	+0.60	1	93068.44	(^{3}P$_2$)6s	[2]$_{5/2}$	111958.89	(^{3}P$_2$)6p	[2]$_{5/2}$	
				+0.45	2,3,4							
				+0.351N								
				+0.382±0.013ZBD								
5309.27	200	5309.27	0.00	−0.95	1,2,3,4	102799.07	(^{3}P$_1$)6s	[1]$_{3/2}$	121628.82	(^{3}P$_0$)6p	[1]$_{3/2}$	
5313.87	800	5313.76	−0.11	−0.10	1	113705.40	(^{3}P$_2$)6p	[3]$_{7/2}$	132518.82	(^{3}P$_2$)7s	[2]$_{5/2}$	
				−0.15	2							
				−0.05	3,4							
5339.33	1000	5339.355	+0.025	−0.07	1,4	93068.94	(^{3}P$_2$)6s	[2]$_{5/2}$	111792.17	(^{3}P$_2$)6p	[2]$_{3/2}$	
				−0.10	2							
				−0.15	3							
				+0.048±0.019ZBD								
5368.07	100	5368.075	+0.005	−1.05	1,2,3	105947.55	(^{3}P$_2$)5d	[0]$_{1/2}$	124571.09	(^{3}P$_1$)6p	[1]$_{1/2}$	
5372.39	300	5372.405	+0.015	−0.211N	1,4	95064.38	(^{3}P$_2$)6s	[2]$_{3/2}$	113672.89	(^{3}P$_2$)6p	[1]$_{1/2}$	blend
				−0.10	2,3							
5419.15	2000	5419.155	+0.005	+0.42	1	95064.38	(^{3}P$_2$)6s	[2]$_{3/2}$	113512.36	(^{3}P$_2$)6p	[3]$_{5/2}$	
				+0.35	2,3,4							
				+0.215N								
				+0.256±0.015ZBD								
5438.96	400	5438.96	0.00	−0.44	1,2,3,4	102799.07	(^{3}P$_1$)6s	[1]$_{3/2}$	121179.80	(^{3}P$_1$)6p	[0]$_{1/2}$	
				−0.183N								
5450.45	100	5450.45	0.00	−1.10	1	105947.55	(^{3}P$_2$)5d	[0]$_{1/2}$	124289.45	(^{3}P$_1$)6p	[1]$_{3/2}$	
				−0.90	2,3							
5460.39	300	5460.365	−0.025	−0.85	1	95396.74	(^{3}P$_2$)5d	[2]$_{5/2}$	113705.40	(^{3}P$_2$)6p	[3]$_{7/2}$	
				−0.75	2,3,4							
				−0.673±0.030ZBD								
5472.61	500	5472.60	−0.01	−0.55	1,2,3,4	95437.67	(^{3}P$_2$)5d	[3]$_{7/2}$	113705.40	(^{3}P$_2$)6p	[3]$_{7/2}$	
				−0.449N								
				−0.362±0.030ZBD								

Table B.1. cont.

λ(Lab)	Int.	λ(stellar)	$\Delta\lambda$	log gf		χ_{low}(cm^{-1})	Term		χ_{up}(cm^{-1})	Term		Notes
5531.07	400	5531.05	−0.02	−0.90	1	95437.67	$(^3P_2)5d$	$[3]_{7/2}$	113512.36	$(^3P_2)6p$	$[3]_{5/2}$	
				−0.80	2,3							
				−0.616N	4							
				−0.632±0.021ZBD								
5616.67	150	5616.65	−0.02	−0.80	1,3,4	105313.33	$(^3P_2)5d$	$[1]_{3/2}$	123112.54	$(^3P_1)6p$	$[2]_{5/2}$	blend
				−0.40	2							
5659.38	150	5659.38	0.00	−0.80	1,3	106906.12	$(^3P_1)6s$	$[1]_{1/2}$	124571.09	$(^3P_1)6p$	$[1]_{1/2}$	
				−0.50	2,4							noise ?
5667.56	300	5667.540	−0.02	−0.65	1	96033.48	$(^3P_2)5d$	$[2]_{3/2}$	113672.89	$(^3P_2)6p$	$[1]_{1/2}$	
				−0.50	2,3							
				−0.45	4							
5699.61	100	5699.61	0.00	−0.85?	1	111326.96	$(^3P_1)5d$	$[2]_{3/2}$	128867.20	$(^1D_2)6p$	$[3]_{5/2}$	2,3,4 noise
5719.61	200	5719.587	−0.023	−0.80	1,2	96033.48	$(^3P_2)5d$	$[2]_{3/2}$	113512.36	$(^3P_2)6p$	$[3]_{5/2}$	3,4 blend telluric
				−0.746N								
				−0.687±0.023ZBD								
5726.91	200	5726.88	−0.03	−0.35	1	114751.08	$(^3P_2)5d$	$[3]_{5/2}$	132207.76	$(^1D_2)6p$	$[2]_{5/2}$	3 blend telluric
				−0.25	2,4							
5751.03	200	5750.99	−0.04	−0.35	1,2	106906.12	$(^3P_1)6s$	$[1]_{1/2}$	124289.45	$(^3P_1)6p$	$[1]_{3/2}$	2 noise
				−0.45	3,4							
5758.65	100	5758.665	+0.015	−0.35	1,4	112703.64	$(^3P_1)5d$	$[2]_{5/2}$	130063.96	$(^1D_2)6p$	$[3]_{7/2}$	blend, 2,3 noise
5776.39	100	5776.39	0.00	−0.70	1	105947.55	$(^3P_2)5d$	$[0]_{1/2}$	123254.60	$(^3P_1)6p$	$[2]_{3/2}$	2,3 not obs, 4 no spectrum
5893.29	150	5893.29	0.00	−0.90	1	112703.64	$(^3P_1)5d$	$[2]_{5/2}$	129667.35	$(^1D_2)6p$	$[1]_{3/2}$	2 noise, 3 not obs, 4 blend
5905.13	200	5905.115	−0.015	−0.85	1	104250.06	$(^3P_1)5d$	$[1]_{1/2}$	121179.80	$(^3P_1)6p$	$[0]_{1/2}$	
				−0.65	2							2,3 blend telluric
5945.53	300	5945.53	0.00	−0.60	2,4	96958.18	$(^3P_2)5d$	$[1]_{1/2}$	113672.89	$(^3P_2)6p$	$[1]_{1/2}$	1 blend telluric
				−0.80	3							
5971.13	200	5971.135	+0.005	−0.50	1	112924.84	$(^1D_2)6s$	$[2]_{3/2}$	129667.35	$(^1D_2)6p$	$[1]_{3/2}$	2,3,4 noise
5976.46	1000	5976.460	+0.00	−0.222N	1,2	95064.38	$(^3P_2)6s$	$[2]_{3/2}$	111792.17	$(^3P_2)6p$	$[2]_{3/2}$	
				−0.35	3,4							
				−0.317±0.023ZBD								
6036.20	500	6036.170	−0.03	−0.57	1	95396.74	$(^3P_2)5d$	$[2]_{5/2}$	111958.89	$(^3P_2)6p$	$[2]_{5/2}$	
				−0.45	2							
				−0.609N	3,4							
				−0.562±0.020ZBD								
6051.15	1000	6051.120	−0.03	−0.252N	1,2,3	95437.67	$(^3P_2)5d$	$[3]_{7/2}$	111958.89	$(^3P_2)6p$	$[2]_{5/2}$	
				−0.35	4							
				−0.257±0.020ZBD								
6097.59	1000	6097.57	−0.02	−0.45	1,3	95396.74	$(^3P_2)5d$	$[2]_{5/2}$	111792.17	$(^3P_2)6p$	$[2]_{3/2}$	
				−0.35	2							
				−0.30	4							
				−0.237N								
				−0.355±0.025ZBD								
6101.43	200	6101.37	−0.06	−0.70	1,4	107904.50	$(^3P_1)5d$	$[1]_{3/2}$	124289.45	$(^3P_1)6p$	$[1]_{3/2}$	2 noise, 4 blend
				−0.10	3							

Table B.1. cont.

λ(Lab)	Int.	λ(stellar)	$\Delta\lambda$	log gf		χ_{low}(cm^{-1})	Term		χ_{up}(cm^{-1})	Term		Notes
6194.07	300	6194.07	0.00	−0.10	1	124070.06	(^{1}D$_2$)5d	[1]$_{3/2}$	140209.99	(^{3}P$_2$)4f	[2]$_{5/2}$	2 noise, 4 blend
				+0.20	3							
6270.82	400	6270.82	−0.01	−0.35	1	112924.84	(^{1}D$_2$)6s	[2]$_{3/2}$	128867.20	(^{1}D$_2$)6p	[3]$_{5/2}$	1 blend, 4 noise
				−0.10	2,3							
				−0.196N								
6277.54	300	−−		−0.894N		96033.48	(^{3}P$_2$)5d	[2]$_{3/2}$	111958.89	(^{3}P$_2$)6p	[2]$_{5/2}$	1,2,3,4 in telluric
				−0.778±0.021ZBD								
6300.86	100	6300.830	−0.03	−1.10	1							2,3,4 noise
6343.96	300	6343.94	−0.02	−0.80	1	96033.48	(^{3}P$_2$)5d	[2]$_{3/2}$	111792.17	(^{3}P$_2$)6p	[2]$_{3/2}$	
				−0.65	2							
		6343.95	−0.01	−0.55	3,4							
				−0.786±0.024ZBD								
6356.35	500	6356.33	−0.02	−0.25	1	124301.96	(^{1}D$_2$)5d	[2]$_{5/2}$	140029.99	(^{3}P$_2$)4f	[4]$_{7/2}$	2,3,4 noise
6375.28	100	6375.28	+0.00	−1.00	1	105947.55	(^{3}P$_2$)5d	[0]$_{1/2}$	121628.82	(^{3}P$_0$)6p	[1]$_{3/2}$	2,3,4 noise
6512.83	300	6512.79	−0.04	−1.00	1,2,3	107904.50	(^{3}P$_1$)5d	[1]$_{3/2}$	123254.60	(^{3}P$_1$)6p	[2]$_{3/2}$	4 blend telluric
6528.65	200	6528.65	+0.00	−0.40	1	114751.08	(^{3}P$_1$)5d	[3]$_{5/2}$	130063.96	(^{1}D$_2$)6p	[3]$_{7/2}$	2,3,4 noise
6595.01	800	6594.97	−0.04	+ 0.00	1,2,3	114905.15	(^{1}D$_2$)5d	[4]$_{9/2}$	130063.96	(^{1}D$_2$)6p	[3]$_{7/2}$	blend, 4 blend telluric
6597.25	300	6597.23	−0.02	−0.60	1,2	106475.21	(^{3}P$_1$)5d	[1]$_{3/2}$	123254.60	(^{3}P$_1$)6p	[2]$_{3/2}$	4 noise
6620.02	200	6620.02	+0.00	−0.85	1,4	105313.33	(^{3}P$_2$)5d	[1]$_{3/2}$	120414.87	(^{3}P$_0$)6p	[1]$_{1/2}$	2,3 noise, 4 blend
6694.32	400	6694.285	−0.035	−1.00	1,2	96858.18	(^{3}P$_2$)5d	[1]$_{1/2}$	111792.17	(^{3}P$_2$)6p	[2]$_{3/2}$	4 noise
				−0.75	3							
				−0.912±0.020ZBD								
6788.71	100	6788.71	0.00	−0.50	1	109653.14	(^{1}D$_2$)6s	[2]$_{5/2}$	124289.45	(^{3}P$_1$)6p	[1]$_{3/2}$	2,4 noise
6790.37	80	6790.37	0.00	−0.70	1	106907.120	(^{3}P$_1$)6s	[1]$_{1/2}$	121628.82	(^{3}P$_0$)6p	[1]$_{3/2}$	2 blend, 3,4 noise
6805.74	1000	− − −				108423.070	(^{3}P$_1$)5d	[3]$_{7/2}$	123112.54	(^{3}P$_1$)6p	[2]$_{5/2}$	1,2,3,4 blend
				−0.595N								
				−0.547±0.023ZBD								
6990.88	2000	6990.835	−0.045	+0.25	1,2	99404.99	(^{3}P$_2$)5d	[4]$_{9/2}$	113705.40	(^{3}P$_2$)6p	[3]$_{7/2}$	
				+0.35	3,4							
				+0.200N								
				+0.084±0.032ZBD								
7082.15	200	7082.15	0.00	+0.05	1	114751.080	(^{3}P$_1$)5d	[3]$_{5/2}$	128867.20	(^{1}D$_2$)6p	[3]$_{5/2}$	2,3 noise, 4 blend
7164.83	800	7164.85	+0.02	+0.20	1,2	114913.98	(^{1}D$_2$)5d	[4]$_{7/2}$	128867.20	(^{1}D$_2$)6p	[3]$_{5/2}$	3,4 blend telluric
7284.34	100	7284.24	−0.10	−0.50	1	107904.50	(^{3}P$_1$)5d	[1]$_{3/2}$	121628.82	(^{3}P$_0$)6p	[1]$_{3/2}$	2,4, 3?? noise
7339.30	300	7339.30	0.00	+0.45	1	108007.28	(^{3}P$_0$)5d	[2]$_{5/2}$	121628.82	(^{3}P$_0$)6p	[1]$_{3/2}$	2,4 noise,3??
7787.04	100	7787.04	0.00	−0.50?	1	119085.49	(^{1}D$_2$)5d	[5]$_{5/2}$	131923.79	(^{1}D$_2$)6p	[5]$_{3/2}$	2,3,4 noise